Species Invasion in a Two-Dimensional Space with Irregularly Shaped Patches

Ankur Jain*

Mechanical and Aerospace Engineering Department
University of Texas at Arlington, Arlington, TX, USA

* – Corresponding Author: email: jaina@uta.edu; Ph: +1 (817) 272-9338
500 W First St, Rm 211, Arlington, TX, USA 76019

CRediT Authorship Contribution Statement

Ankur Jain – Conceptualization, Methodology, Formal Analysis, Investigation, Data Curation, Visualization, Writing Original Draft, Review/Editing.

Abstract:

Accounting for spatial heterogeneity in the evolution of a species population in a given space is of much importance in population ecology, epidemiology and related fields in biosciences. Past literature has presented such analysis in the presence of regions with distinct diffusion/growth properties, often referred to as patches. However, most of the past work is limited to one-dimensional space, whereas in practice, population evolution occurs in two dimensions, and realistic patches may have irregular shapes. This work addresses this limitation by deriving an exact analytical solution for a linear diffusion-reaction population growth problem in two-dimensional space containing an arbitrary number of irregularly shaped patches. The spatial variation in diffusion/growth coefficients is represented using Heaviside functions, and an exact expression for the transient coefficient functions in the series solution is derived. A threshold condition for establishment of the population at large time is derived. Results from this work are shown to reduce to well-known results for simpler problems under limiting conditions. Based on the technique, extinction and establishment regions in the parameter space are identified. A number of illustrative problems containing patches of irregular shapes, such as heart-shaped and leaf-shaped patches are solved in order to demonstrate the versatility of the technique. This work contributes a novel mathematical tool for solving population dynamics problems in realistic conditions, including irregular patch shapes, with potential applications in a number of problems in ecology and epidemiology.

Keywords: Population Dynamics; Population Ecology; Epidemiology; Diffusion-Reaction Partial Differential Equation.

Nomenclature

L, W	Outer dimensions of the 2D Cartesian body
c	population density (m^{-2})
D	diffusion coefficient (m^2s^{-1})
$\overline{D}$	non-dimensional diffusion coefficient
$\mathcal{H}$	Heaviside step function
N	number of terms
$\mathbb{N}$	eigenfunction norm
$\wp$	total number of oasis/deadzone regions/patches
$\wp_{in}$	total number of initial population regions
r	growth coefficient (s^{-1})
$\bar{r}$	non-dimensional growth coefficient
t	time (s)
x, y	Cartesian coordinates (m)
x_{1p}, x_{2p}	x direction lower and upper limits of p^{th} region (m)
y_{1p}, y_{2p}	y direction lower and upper limits of p^{th} region, both as functions of x (m)
λ, μ	Spatial eigenfunctions
Δ	determinant
δ	Dirac delta function
ϕ	Kronecker delta
ξ, η	Non-dimensional Cartesian coordinates
τ	Non-dimensional time
ξ_{1p}, ξ_{2p}	non-dimensional ξ direction lower and upper limits of p^{th} region
η_{1p}, η_{2p}	non-dimensional η direction lower and upper limits of p^{th} region, both as functions of ξ

Subscripts

in	initial
p	region number
tot	total
0	Background region outside the oasis/deadzone patches

1. Introduction

Determining the spatiotemporal dynamics of population density of a species in a given space is an important problem in mathematical ecology [1-4], with applications in several practical scenarios such as spreading of invasive species [5], ecological preservation [6], harvesting [7] and resource planning [8]. The primary motivation of such analysis is often to determine, given the nature of diffusion, growth and other relevant processes, whether the species eventually establishes itself within the space or goes extinct. Such problems have been studied mathematically for a long time [9-13]. In general, the evolution of population density of a species in a given space may be driven by a combination of diffusion, growth – which may be either positive or negative – as well as advective effects. In addition, conditions at the boundaries of the space [14], aspect ratio of the space (if two-dimensional) [10], and the fragmentation of growth regions [4,14] also play important roles in determining establishment or extinction of the population. In addition to single species problems, there has also been long-standing interest in two-species problems such as predator-prey systems [15,16]. The literature on a variety of models for these phenomena and their interactions with each other has been well summarized in recent books [4,6].

The diffusion-reaction framework used to study such population dynamics problems also finds applications in other fields, such as epidemiology [1] and proliferation of cancer cells [17]. Additionally, several engineering processes such as stability of thermal systems [18], heat transfer in power electronic devices [19], contaminant transport [20] and drug delivery [21] are also governed by a similar set of equations.

Spatiotemporal dynamics of population density is commonly modeled using the Kierstead-Slobodkin-Skellam (KISS) diffusion-reaction model [9,10], which, for a simple homogeneous one-dimensional problem may be written as

$$\frac{\partial c}{\partial t} = D\frac{\partial^2 c}{\partial x^2} + F(c) \quad (1)$$

where $c(x,t)$ is the population density distribution D is the diffusion coefficient and $F(c)$ is the growth term. A variety of models for $F(c)$ have been used, including Malthusian growth, logistic growth and the Allee effect [6]. Asocial phenomena related to negative growth at low population density have also been studied [22]. Amongst these models, the linear Malthusian growth model $F(c) = rc$, where r is the growth coefficient, is of particular interest due to the resulting simplification in analysis and possibility of deriving an exact analytical solution. An additional convective term has also been considered in equation (1) for modeling advective transport, for example, that of insects due to wind [23]. In addition to such deterministic approaches, stochastic analysis of diffusion-reaction processes has been reported [24]. Numerical calculation of population growth has also been carried out in scenarios where exact analysis is difficult [25]. More recently, machine learning based analysis of diffusion-reaction processes has also been reported [26].

A topic of specific interest in the mathematical study of population dynamics has been in understanding the effect of spatial heterogeneity [27]. Such heterogeneity may be in the form of discrete regions within the space, often referred to as patches [14,28,29] that have different diffusion and/or growth properties than the rest of the space. Discrete heterogeneity in the initial distribution of the population within the space also occurs commonly, for example, when the population is initially seeded only in specific regions. Results related to single [29], two [30] or an arbitrary number of patches [14] in a one-dimensional space are available. The general technique to address such problems has been to derive expressions for population density distributions in each patch separately and determine series coefficients in order to satisfy interface

conditions between patches [14]. While the matching of population density and flux are the most common interface conditions, other formulations have also been used for modeling more advanced interactions between patches [15,30]. Through such analysis, the effect of number of patches, their locations and relative growth coefficients on population dynamics and eventual establishment/extinction has been studied [14,29].

Most mathematical models for population dynamics in heterogeneous space are limited to one-dimensional geometry [14,28,29,30], where each patch represents a sub-section of the entire length of the space under consideration. While this simplifies analysis significantly, and helps understand the fundamentals of the problem, nevertheless, such one-dimensional representation may not be sufficiently accurate for practical problems where the population usually spreads over a two-dimensional space. In principle, the one-dimensional analysis summarized above is extendable to two-dimensional space by considering both sets of eigenvalues coming from two orthogonal directions, however, such an approach can only account for patches of specific shapes. For example, an extension of the 1D work described above to a two-dimensional Cartesian space only works if the patches are rectangular. However, it has been pointed out [6] that in practice, patches are not necessarily rectangular, and may have irregular shape. Accounting for the irregular shape of such regions/patches is an important need for mathematical modeling of realistic population dynamics processes.

This work presents a mathematical technique for solving the linear diffusion-reaction equation in a two-dimensional space containing a number of irregularly shaped regions/patches, each with discrete diffusion and growth coefficients, as shown in Figure 1. The method is based on representing the spatial variation of diffusion and growth coefficients due to the two-dimensional shape of patches using Heaviside functions. By doing so, an exact expression for the

transient coefficient functions in the series solution for the population density distribution is derived. An exact threshold condition to determine whether establishment of the population occurs or not is derived in terms of the determinant of a matrix. A number of example problems containing multiple patches of irregular two-dimensional shapes are solved to illustrate the versatility of the technique developed here. The next section defines the mathematical problem of interest, introduces the Heaviside functions based representation of spatial variation of diffusion/growth coefficients, and presents a technique for solving this problem. The main result related to a criterion for population establishment is presented in Section 3. A detailed discussion of key results based on the theoretical technique are presented in Section 4, followed by concluding remarks in Section 5.

2. Methods

2.1. Problem Definition and Non-Dimensionalization

This problem considered here involves spatiotemporal dynamics of population density of a species in a finite two-dimensional Cartesian space of size L by W, as shown in Figure 1. In addition to diffusive transport, population growth occurs in an arbitrary number of irregularly-shaped regions based on a linear Malthusian model [6]. A linear growth model simplifies analysis and provides an upper bound for the solution to the more general non-linear problem [6]. The boundaries of the two-dimensional Cartesian space are assumed to be hostile to the species, so that the species concentration at the boundaries always remains zero. The population is initially located only in specific discrete regions within the space. Based on a balance between the rate of increase in population due to growth, reduction due to hostile boundaries and spatial redistribution due to diffusion, the interest is in determining whether the population ultimately establishes itself in the two-dimensional space or goes extinct.

As shown in Figure 1, a key feature of the model presented here is that there may be $\wp$ irregularly shaped regions within the two-dimensional space, each with its own uniform diffusion and growth coefficients. The growth coefficient in the p^{th} region is denoted by r_p, whereas the growth coefficient outside these regions is denoted by r_0. The growth coefficient may be positive, i.e., the region may be conducive to population growth (referred to as an oasis in this work), or may be negative, i.e., the region may be hostile to population growth (referred to as a deadzone in this work). Similarly, the diffusion coefficient within the p^{th} region is denoted by D_p and outside the regions by D_0. All diffusion and growth coefficients are assumed to be uniform within each region and invariant with population density, so that second-order effects such as the Allee effect that cause non-linearity are neglected. In addition, the diffusion coefficients are assumed to be isotropic, so that there is no preferred direction for diffusion.

The arbitrary shape of the p^{th} oasis/deadzone region is mathematically defined by lower and upper bounds x_{1p} and x_{2p} in the x direction and, further, by functions $y_{1p}(x)$ and $y_{2p}(x)$ that represent the lower and upper bounds of the shape in the y direction, which are both, in general, functions of x. For example, for a circular-shaped oasis region center of radius R and centered at (x_0, y_0), $x_{1p} = x_0 - R$, $x_{2p} = x_0 + R$, $y_{1p}(x) = y_0 - \sqrt{R^2 - (y - y_0)^2}$ and $y_{2p}(x) = y_0 + \sqrt{R^2 - (x - x_0)^2}$. Based on these geometrical definitions, the growth regions, as well as the regions of initial population may have nearly arbitrary non-Cartesian shapes within the Cartesian space.

Further, the initial distribution of the population in the two-dimensional region is also assumed to be discrete in $\wp_{in}$ regions, where the p^{th} region has an initial population density of $c_{in,p}$ and, similar to the oasis/deadzone regions, is located between $x_{1in,p}$ and $x_{2in,p}$ in the x

direction and $y_{1in,p}(x)$ and $y_{2in,p}(x)$ in the y direction. It is assumed that there is no population initially present outside these $\wp_{in}$ regions. In general, as shown in Figure 1, the $\wp$ oasis/deadzone regions and the $\wp_{in}$ regions of initial population distribution may be different from each other.

Based on this problem definition above, the goal of this work is to mathematically formulate and solve a multi-region diffusion-reaction problem in order to determine the population density distribution as a function of space and time. Specifically, given the values of various geometrical, diffusion and growth parameters, it is of interest to determine how the species evolves over time, and whether there is establishment or extinction of the species at large time.

Since each oasis/deadzone region has different values of the diffusion and growth parameters, therefore, the diffusion-reaction equation may be written for each region, along with interface conditions at the boundaries of each region. While such an approach has been reported for one-dimensional geometry [14,28,29], doing so in two-dimensional space, especially satisfying the interface conditions between regions and the background, is extremely difficult and cumbersome due to the arbitrary geometry of each region. As a simple example, satisfying interface conditions along the boundaries of a circular oasis region located inside a two-dimensional rectangular space is mathematically very complicated. Instead, the technique used in this work writes the conservation equation and solves it for a single function $c(x, y, t)$ that represents the population density through the entire two-dimensional space, including all growth regions. Within this framework, the transient species conservation equation accounting for diffusion and growth may be written as

$$\frac{\partial}{\partial x}\left(D(x,y)\frac{\partial c}{\partial x}\right)+\frac{\partial}{\partial y}\left(D(x,y)\frac{\partial c}{\partial y}\right)+r(x,y)\cdot c=\frac{\partial c}{\partial t}\qquad(0<x<L,0<y<W,t>0) \tag{2}$$

where the spatial functions $D(x,y)$ and $r(x,y)$ must represent the discrete variation of the diffusion coefficient and growth coefficient, respectively, within the two-dimensional space. $D(x,y)$ and $r(x,y)$ must be defined in order to correctly account for the distinct values of the diffusion and growth coefficients within each oasis/deadzone region (D_p and r_p, respectively, in the p^{th} region), as well as in the background outside the regions (D_0 and r_0, respectively). This is accomplished by the use of the Heaviside step function as follows:

$$D(x,y)=D_0+\sum_{p=1}^{\wp}\left(D_p-D_0\right)\left(\mathcal{H}\left(x-x_{1p}\right)-\mathcal{H}\left(x-x_{2p}\right)\right)\left(\mathcal{H}\left(y-y_{1p}(x)\right)-\mathcal{H}\left(y-y_{2p}(x)\right)\right) \tag{3}$$

Note that $\mathcal{H}$ denotes the Heaviside step function [31], which represents a step change at a certain location, defined as $\mathcal{H}(x-a)=1$ if $x>a$, and 0 if $x<a$. The definition of $D(x,y)$ provided by equation (3) makes use of the difference between two Heaviside functions in each direction, which effectively produces a top hat function. The product of the two top hat functions in equation (3) ensures, based on the definition of parameters x_{1p}, x_{2p}, $y_{1p}(x)$ and $y_{2p}(x)$ for each region, that $D(x,y)=D_p$ inside the p^{th} region (i.e., when $x_{1p}<x<x_{2p}$ and $y_{1p}(x)<y<y_{2p}(x)$) and $D(x,y)=D_0$ outside the oasis/deadzone regions. Similarly, the growth coefficient function may be expressed as

$$r(x,y) = r_0 + \sum_{p=1}^{\wp} (r_p - r_0)\left(\mathcal{H}(x - x_{1p}) - \mathcal{H}(x - x_{2p})\right)\left(\mathcal{H}(y - y_{1p}(x)) - \mathcal{H}(y - y_{2p}(x))\right) \quad (4)$$

The boundary conditions associated with this problem are simply $c = 0$ at $x = 0, L$ and at $y = 0, W$. The initial condition associated with this problem may be written mathematically as

$$c = c_{in}(x,y) \qquad (t = 0) \quad (5)$$

where the spatial function $c_{in}(x,y)$ must account for the discrete distribution of the initial population in the $\wp_{in}$ regions. Similar to the diffusion and growth coefficients, $c_{in}(x,y)$ may be expressed using Heaviside functions as follows:

$$c_{in}(x,y) = \sum_{p=1}^{\wp_{in}} c_{in,p}\left(\mathcal{H}(x - x_{1in,p}) - \mathcal{H}(x - x_{2in,p})\right)\left(\mathcal{H}(y - y_{1in,p}(x)) - \mathcal{H}(y - y_{2in,p}(x))\right) \quad (6)$$

This definition ensures that the initial population distribution is uniformly $c_{in,p}$ inside the p^{th} region in which the population is initially located, and is zero outside these regions.

It is of interest to solve equation (2) based on the definitions of coefficient functions given by equations (3) and (4), and the initial condition given by equation (5), along with zero population boundary conditions. Due to the large number of variables and parameters involved in this general problem, it is helpful to carry out a non-dimensionalization of the problem first. The following non-dimensional parameters are introduced:

$$\bar{c} = \frac{c}{c_{ref}};\ \xi = \frac{x}{L};\ \eta = \frac{y}{L};\ \tau = \frac{D_0 t}{L^2};\ \bar{W} = \frac{W}{L};\ \xi_{1p} = \frac{x_{1p}}{L};\ \xi_{2p} = \frac{x_{2p}}{L};\ \eta_{1p} = \frac{y_{1p}}{L};\ \eta_{2p} = \frac{y_{2p}}{L};\ \bar{D}_p = \frac{D_p}{D_0};\ \bar{r}_p = \frac{r_p L^2}{D_0};\ \bar{r}_0 = \frac{r_0 L^2}{D_0};\ \bar{c}_{in,p} = \frac{c_{in,p}}{c_{ref}} \tag{7}$$

where c_{ref} is a reference population density. In case of a single region initially populated region, its population density may be conveniently used as the reference population density.

Based on this, the non-dimensional population density problem may be written as

$$\frac{\partial}{\partial \xi}\left(\bar{D}(\xi,\eta)\frac{\partial \bar{c}}{\partial \xi}\right) + \frac{\partial}{\partial \eta}\left(\bar{D}(\xi,\eta)\frac{\partial \bar{c}}{\partial \eta}\right) + \bar{r}(\xi,\eta)\cdot\bar{c} = \frac{\partial \bar{c}}{\partial \tau} \qquad (0 < \xi < 1, 0 < \eta < \bar{W}, \tau > 0) \tag{8}$$

where

$$\bar{D}(\xi,\eta) = 1 + \sum_{p=1}^{\wp}\left(\bar{D}_p - 1\right)\left(\mathcal{H}\left(\xi - \xi_{1p}\right) - \mathcal{H}\left(\xi - \xi_{2p}\right)\right)\left(\mathcal{H}\left(\eta - \eta_{1p}(\xi)\right) - \mathcal{H}\left(\eta - \eta_{2p}(\xi)\right)\right) \tag{9}$$

and similar equations for $\bar{r}(\xi,\eta)$ and $\bar{c}_{in}(\xi,\eta)$.

2.2. Solution Methodology

In order to derive a solution for this general problem, the population density distribution $\bar{c}(\xi,\eta,\tau)$ is expressed as follows

$$\bar{c}(\xi,\eta,\tau)=\sum_{n=1}^{\infty}\sum_{m=1}^{\infty}A_{nm}(\tau)f_n(\xi)g_m(\eta) \tag{10}$$

where $f_n(\xi)$ and $g_m(\eta)$ are eigenfunctions in the ξ and η directions, respectively. Based on the zero population boundary conditions assumed in this work, $f_n(\xi)=\sin(\lambda_n\xi)$ and $g_m(\xi)=\sin(\mu_m\xi)$, where $\lambda_n=n\pi$ and $\mu_m=m\pi/\bar{W}$ are the eigenvalues.

The coefficients $A_{nm}(\tau)$ account for the changes in the population density distribution over time, and must be determined from equation (8) and the associated initial condition. In order to do so, equation (8) is differentiated by parts, resulting in

$$\bar{D}\left(\frac{\partial^2\bar{c}}{\partial\xi^2}+\frac{\partial^2\bar{c}}{\partial\eta^2}\right)+\frac{\partial\bar{D}}{\partial\eta}\frac{\partial\bar{c}}{\partial\eta}+\frac{\partial\bar{D}}{\partial\xi}\frac{\partial\bar{c}}{\partial\xi}+\bar{r}\cdot\bar{c}=\frac{\partial\bar{c}}{\partial\tau} \tag{11}$$

Further, using the series solution for the population density given by equation (10) into equation (11), the following equation may be derived:

$$\begin{aligned}\frac{\partial\bar{D}}{\partial\xi}\sum_{n=1}^{\infty}\sum_{m=1}^{\infty}A_{nm}(\tau)f_n'(\xi)g_m(\eta)-\bar{D}\sum_{n=1}^{\infty}\sum_{m=1}^{\infty}(\lambda_n^2+\mu_m^2)A_{nm}(\tau)f_n(\xi)g_m(\eta)\\+\frac{\partial\bar{D}}{\partial\eta}\sum_{n=1}^{\infty}\sum_{m=1}^{\infty}A_{nm}(\tau)f_n(\xi)g_m'(\eta)+\bar{r}\sum_{n=1}^{\infty}\sum_{m=1}^{\infty}A_{nm}(\tau)f_n(\xi)g_m(\eta)\\=\sum_{n=1}^{\infty}\sum_{m=1}^{\infty}A_{nm}'(\tau)f_n(\xi)g_m(\eta)\end{aligned} \tag{12}$$

From equation (9), the derivatives of $\bar{D}$ appearing in equation (12) may be written as follows:

$$\frac{\partial \bar{D}}{\partial \xi} = \sum_{p=1}^{\wp} (\bar{D}_p - 1)\left(\delta(\xi - \xi_{1p}) - \delta(\xi - \xi_{2p})\right)\left(\mathcal{H}(\eta - \eta_{1p}(\xi)) - \mathcal{H}(\eta - \eta_{2p}(\xi))\right)$$
$$+ \sum_{p=1}^{\wp} (\bar{D}_p - 1)\left(\mathcal{H}(\xi - \xi_{1p}) - \mathcal{H}(\xi - \xi_{2p})\right)\left(\delta\left(\eta - \eta_{2p}(x)\right)\eta'_{2p}(\xi)\right. \quad (13)$$
$$\left. - \delta\left(\eta - \eta_{1p}(\xi)\right)\eta'_{1p}(\xi)\right)$$

$$\frac{\partial \bar{D}}{\partial \eta} = \sum_{p=1}^{\wp} (\bar{D}_p - 1)\left(\mathcal{H}(\xi - \xi_{1p}) - \mathcal{H}(\xi - \xi_{2p})\right)\left(\delta(\eta - \eta_{1p}(\xi)) - \delta(\eta - \eta_{2p}(\xi))\right) \quad (14)$$

Equations (13) and (14) use the following property of Heaviside functions: $\frac{d}{dx}\left(\mathcal{H}(x - x^*)\right) = \delta(x - x^*)$, where δ is the Dirac delta function [31].

Equation (12) is then multiplied by $f_i(x)g_j(y)$ for each $i = 1,2..\infty$ and $j = 1,2..\infty$, followed by integration over the entire region and some mathematical rearrangement. In particular, integrals involving Dirac delta functions are simplified using the following integral property of Dirac delta functions related to a general function $F(x)$: $\int_{-\infty}^{\infty} \delta(x - x^*)F(x)dx = F(x^*)$. This leads to the following set of linear ordinary differential equations

$$\mathbb{N}_{x,i}\mathbb{N}_{y,j}A'_{ij}(\tau) = \sum_{n=1}^{\infty}\sum_{m=1}^{\infty}\left(I_{1nmij} - (\lambda_n^2 + \mu_m^2)I_{2nmij} + I_{3nmij} + I_{4nmij}\right)A_{nm}(\tau) \quad (15)$$

where

$$I_{1nmij} = \sum_{p=1}^{\wp} (\bar{D}_p - 1) \int_{\xi_{1p}}^{\xi_{2p}} f_n'(\xi) f_i(\xi) \left[\eta_{2p}'(\xi) g_m\left(\eta_{2p}(\xi)\right) g_j\left(\eta_{2p}(\xi)\right) - \eta_{1p}'(\xi) g_m(\eta_{1p}(\xi)) g_j(\eta_{1p}(\xi)) \right] d\xi \tag{16}$$

$$I_{2nmij} = \phi_{ni}\phi_{mj}\mathbb{N}_{x,i}\mathbb{N}_{y,j} + \sum_{p=1}^{\wp} (\bar{D}_p - 1) \int_{\xi_{1p}}^{\xi_{2p}} f_n(\xi) f_i(\xi) \left[\int_{\eta_{1p}(\xi)}^{\eta_{2p}(\xi)} g_m(\eta) g_j(\eta) d\eta \right] d\xi \tag{17}$$

$$I_{3nmij} = \sum_{p=1}^{\wp} (\bar{D}_p - 1) \int_{\xi_{1p}}^{\xi_{2p}} f_n(\xi) f_i(\xi) \left[g_m'(\eta_{1p}(\xi)) g_j\left(\eta_{1p}(\xi)\right) - g_m'(\eta_{2p}(\xi)) g_j\left(\eta_{2p}(\xi)\right) \right] d\xi \tag{18}$$

$$I_{4nmij} = \bar{r}_0\phi_{ni}\phi_{mj}\mathbb{N}_{x,i}\mathbb{N}_{y,j} + \sum_{p=1}^{\wp} (\bar{r}_p - \bar{r}_0) \int_{\xi_{1p}}^{\xi_{2p}} f_n(\xi) f_i(\xi) \left[\int_{\eta_{1p}(\xi)}^{\eta_{2p}(\xi)} g_m(\eta) g_j(\eta) d\eta \right] d\xi \tag{19}$$

where $\mathbb{N}_{x,i} = 1/2$ and $\mathbb{N}_{y,j} = \bar{W}/2$ are the eigenfunction norms, and ϕ_{ni} represents the Kronecker delta function, such that $\phi_{ni} = 1$ if $n = i$ and 0 otherwise.

Note that for the case of zero population boundary conditions assumed in this work, the functions $f_n(\xi)$ and $g_m(\eta)$ are both straightforward sinusoidal functions, the integrals of which appearing in equations (16)-(19) may be easily determined.

Equation (15) may be written compactly as a first-order matrix ordinary differential equation (ODE) as follows

$$\boldsymbol{A}'(t) = \boldsymbol{M}\boldsymbol{A}(t) \tag{20}$$

where the vector $\boldsymbol{A}(t)$ comprises the functions $A_{ij}(t)$, and the size of $\boldsymbol{A}(t)$ depends on the number of terms in the infinite series considered for computation. The elements of matrix $\boldsymbol{M}$ are defined by equations (15)-(19). A solution for this problem may be written as

$$\boldsymbol{A}(t) = \boldsymbol{A}(0)\exp(\boldsymbol{M}t) \tag{21}$$

where $\boldsymbol{A}(0)$ is the initial value vector that contains the initial values of the coefficients, $A_{ij}(0)$, which may be obtained by multiplying the non-dimensional form of equation (6) by $f_i(\xi)g_j(\eta)$ for each $i = 1,2..\infty$ and $j = 1,2..\infty$, followed by integration over the entire region. This may be shown to result in

$$A_{ij}(0) = \frac{1}{\mathbb{N}_{x,i}\mathbb{N}_{y,j}} \sum_{p=1}^{\wp_{in}} \bar{c}_{in,p} \int_{\xi_{1p}}^{\xi_{2p}} f_n(\xi) \left(\int_{\eta_{1p}(\xi)}^{\eta_{2p}(\xi)} g_m(\eta) d\eta \right) d\xi \tag{22}$$

This completes the solution of the problem. In addition to the detailed population density distribution $\bar{c}(\xi, \eta, \tau)$, a practical quantity of interest may be the total population in the space as a function of time. This quantity, denoted by $\bar{c}_{tot}(\tau)$, may be obtained easily by spatially integrating equation (10), which results in

$$\bar{c}_{tot}(\tau) = \sum_{n=1}^{\infty} \sum_{m=1}^{\infty} A_{nm}(\tau) \frac{1 - \cos(\lambda_n)}{\lambda_n} \frac{1 - \cos(\mu_m \bar{W})}{\mu_m} \tag{23}$$

$\bar{c}_{tot}(\tau)$ may be tracked as a function of time to determine whether the population establishes itself, and if so, how long it takes to establish itself.

Note that the expression for the transient population density distribution derived in this work is exact, since no approximations are made in the derivation of the solution. In particular, the

Heaviside functions based representation of discrete distributions of diffusion and growth coefficient is exact. The solution derived is an infinite series, as is the common case for most diffusion and diffusion-reaction problems in a finite domain.

Note that the functions $\eta_{1p}(\xi)$ and $\eta_{2p}(\xi)$ play a key role in the solution of the problem. These functions represent the shape of the p^{th} oasis/deadzone region. These functions are known in advance through the known shape of each oasis/deadzone region. The derivatives of $\eta_{1p}(\xi)$ and $\eta_{2p}(\xi)$ also appear in the solution and help account for the curvature of the shape of each oasis/deadzone region.

3. Results

A common goal of diffusion-reaction analysis of population growth problems is to determine whether the species will establish itself or go extinct [6]. In this case, the positive growth coefficient in the oasis regions as well as in regions outside the oases, if present, contributes towards growing the population and thus helping it establish itself. On the other hand, diffusion towards the zero population boundaries, as well as the negative growth coefficient in the deadzone regions, if present, both contribute towards extinction. Whether the species establishes itself or goes extinct depends on which of these opposing effects dominates over the other. From a mathematical perspective, whether the population density decays to zero (extinction) or increases exponentially (establishment) at large time depends on whether the coefficients $A_{nm}(\tau)$ are bounded or not as $\tau \to \infty$. It is well known [32] that the elements of a matrix governed by a first-order matrix differential such as (21) are bounded at large times if and only if all eigenvalues of the matrix $\boldsymbol{M}$ have a negative real part. Therefore, a limiting condition for population establishment may be expressed in terms of at least one eigenvalue of the matrix $\boldsymbol{M}$ becoming zero. Finally, since

the determinant of a matrix with a zero eigenvalue is zero, therefore, one may conclude that the threshold condition for establishment of the species at large time is given by the matrix $\boldsymbol{M}$ having zero determinant. For example, as the growth coefficient $\bar{r}$ is increased, the first value of $\bar{r}$ at which the determinant of $\boldsymbol{M}$ becomes zero is the threshold value, beyond which, population establishment will occur, and below which, the population will go extinct at large times. Note that this result only predicts establishment at large times, and does not necessarily address how long it takes to establish. However, this can be easily done by plotting the total population in the space, given by equation (23), as a function of time.

4. Discussion

Since the solution for the population density distribution is obtained in the form of an infinite series, it is first important to determine the minimum number of terms needed to be considered for reasonable accuracy. It is found that the use of 15 terms results in reasonable convergence, in that the predicted population density does not change appreciably (within 1%) by further increase in the number of terms. Eigenfunction based series solution typically need a larger number of terms to small times. In the present problem, the focus is on predicting population density at large times, and, therefore, the number of terms to be considered is not as stringent. All results discussed in this section are computed with 15 terms in the series solution, for which, the integrals appearing in equation (16)-(19) are computed in less than 15 seconds on a standard desktop computer. The computational cost can potentially be reduced with further computational optimization, which has not been carried out here.

4.1. Comparison with Past Work for Special Case of Homogeneous Space

It is of interest to examine the nature of the results obtained here for a special case that has been presented in the past. Specifically, the present work accounts for discrete regions with growth coefficients and diffusion coefficients that may be different from the rest of the two-dimensional space, represented non-dimensionally by $\bar{r}_p$ and $\overline{D}_p$, respectively. The special case of a homogeneous two-dimensional space has been solved in the past [6,10], and the minimum value of the growth coefficient needed for species establishment has been shown to be given by $\bar{r}_{min} = \lambda_1^2 + \mu_1^2 = \pi^2(1 + \overline{W}^{-2})$. It is of interest to examine whether the present work is consistent with this result for this special case, i.e., whether setting the parameter values in the present work to mimic a homogeneous space leads to the result reported in past work. Specifically, in the present framework, the entire two-dimensional region becomes homogeneous when $\bar{r}_p = \overline{D}_p = 1$, i.e., each oasis/deadzone has the same growth coefficient and the same diffusion coefficient as the rest of the space. In order to examine the results from this work in this limit, Figure 2 plots $\bar{r}_{min}$, the minimum value of the growth coefficient needed for population establishment in a problem with a single circular oasis as a function of $\bar{r}_1$, the ratio of growth coefficient in the oasis and the background, while keeping $\overline{D}_1 = 1.0$ and $\overline{W} = 1.5$. $\bar{r}_1 = 1.0$ corresponds to the special case of a homogeneous space, for which, based on past work, $\bar{r}_{min} = 14.256$ for the assumed value of $\overline{W}$. Using these results in Section 2, the minimum value of the growth coefficient is determined as a function of $\bar{r}_1$ by obtaining the value at which the determinant first becomes zero. Figure 2 considers both $\bar{r}_1 < 1$ and $\bar{r}_1 > 1$ regimes, and shows that in both cases, as $\bar{r}_1$ approaches a value of one, the minimum growth coefficient needed for population establishment approaches the expected of 14.256 based on past work. This shows that the present work is consistent with predictions from past work for the special case of a homogeneous two-dimensional space.

It may also be shown mathematically that the present work reduces to past results when the two-dimensional space becomes homogeneous, i.e., when $\bar{r}_p = \bar{D}_p = 1$. In such a case, equations (16)-(19) show that $I_{1nmij} = I_{3nmij} = 0$, $I_{2nmij} = \phi_{ni}\phi_{mj}\mathbb{N}_{x,i}\mathbb{N}_{y,j}$ and $I_{4nmij} = \bar{r}_0\phi_{ni}\phi_{mj}\mathbb{N}_{x,i}\mathbb{N}_{y,j}$. This implies that matrix $\boldsymbol{M}$ is a diagonal matrix, and the differential equation for the coefficients may be written simply as $A'_{ij}(\tau) = \left(\bar{r}_0 - \lambda_i^2 - \mu_j^2\right)\mathbb{N}_{x,i}\mathbb{N}_{y,j}A_{ij}(\tau)$. A straightforward solution for this uncoupled ODE is $A_{ij}(\tau) = A_{ij}(0)\exp\left(\left(\bar{r}_0 - \lambda_i^2 - \mu_j^2\right)\mathbb{N}_{x,i}\mathbb{N}_{y,j}\tau\right)$. This expression, as well as resulting condition for population establishment, $\bar{r}_{0,min} = \lambda_1^2 + \mu_1^2$ is identical to previously reported work on a homogeneous two-dimensional space. This shows that the general model presented in this work, which is capable of accounting for multiple oasis/deadzone regions of arbitrary shape, correctly reduces to the well-known result pertaining to a homogeneous space when the oasis/deadzone regions are taken to have the same growth/diffusion properties as the rest of the space.

4.2. Determinant as an indicator of establishment or extinction

A key result discussed in sections 2 and 3 is that a zero value of the determinant of the matrix $\boldsymbol{M}$ defined by equation (15)-(19) indicates change from extinction to establishment. In general, the value of the determinant, and, therefore, the criterion for species establishment depends on the growth coefficients $\bar{r}_0$ and $\bar{r}_p$, diffusion coefficients $\bar{D}_p$, aspect ratio $\bar{W}$, and the shapes of oasis regions represented by ξ_{1p}, ξ_{2p}, $\eta_{1p}(\xi)$ and $\eta_{2p}(\xi)$ for $p = 1,2,..\wp$. Notably, the shape and size of the initial population regions does not influence eventual establishment or extinction of the species.

In order to illustrate this result in the context of the growth coefficient, a representative problem with two oasis regions and one initial population region is considered. The first oasis is a circle of non-dimensional radius 0.2 centered at $(0.7,0.7)$ and the second oasis is an ellipse centered at $(0.5,1.2)$, with major and minor axes values of $2a = 0.6$ and $2b = 0.4$ along the x and y directions, respectively. The initial population is located in a rectangle of dimensions 0.2 and 0.4 in the the x and y directions, respectively, and centered at $(0.3,0.4)$. Other problem parameters are $\bar{D}_1 = \bar{D}_2 = 1.5$, $\bar{r}_0 = 5$, $\bar{W} = 1.5$. For this problem, the determinant of the matrix $\boldsymbol{M}$ is computed as a function of $\bar{r}$, the growth coefficient in both oasis regions. Figure 3 shows that the determinant has a negative value at small $\bar{r}$. As expected from the discussion in section 3, the determinant curve rises upwards as $\bar{r}$ increases, and eventually crosses the $\bar{r}$ axis at around $\bar{r} = 34$. This shows that $\bar{r} = 34$ is the threshold for species establishment. If the growth coefficient in the oasis regions is lower than this value, the effect of diffusion to the hostile boundaries dominates over species growth in the oasis regions, resulting in species extinction at large times. In contrast, when $\bar{r} > 34$, the rate of population growth in the oasis regions is strong enough to overcome population loss and lead to eventual establishment of the population. Computing the determinant of the matrix $\boldsymbol{M}$ is, therefore, a straightforward method for predicting the establishment vs. extinction characteristics of the problem. Such prediction of establishment-vs-extinction is otherwise not straightforward to do, especially considering the complicated geometry of the problem, including the non-Cartesian shapes of the oasis regions. Based on the discussion in Section 2, oasis regions of any other shapes may also be accounted for in the theoretical model developed here.

While not plotted here beyond $\bar{r} = 50$, the determinant plot is not necessarily monotonic, and may change directions to cross the $\bar{r}$ axis again. However, for the purposes for predicting the

384 threshold for population establishment, only the first root of the determinant curve is of interest
385 because, if the population is shown to establish at a certain value of $\bar{r}$, then, clearly, it will establish
386 itself for larger values of $\bar{r}$ as well.

387 Similar determinant curves as functions of other parameters may also be computed in order
388 to determine the extinction vs. establishment threshold vis-à-vis other parameters, such as
389 diffusion coefficients and sizes of oasis regions. For example, keeping other parameters constant,
390 computing the determinant as a function of oasis size can help determine the minimum oasis size
391 needed for the population to establish itself.

392 In order to further confirm the extinction vs. establishment prediction based on the value
393 of the determinant, the total population in the region $\bar{c}_{tot}$, defined by equation (23), is plotted as a
394 function of time in Figure 4. Curves are presented for two values of $\bar{r}$ below and two values of $\bar{r}$
395 above the predicted threshold of $\bar{r} = 34$ for establishment. Figure 4 clearly shows that $\bar{r} = 10$ and
396 $\bar{r} = 30$ result in steady reduction in population over time, leading to extinction. In contrast, when
397 $\bar{r} = 50$ or $\bar{r} = 60$, the population grows exponentially with time. In both cases, there is a
398 significant time period initially, during which, there is no appreciable rise in population. This is
399 attributed to the time taken for a significant amount of population to diffuse from the initial
400 population region to the two oasis regions, before growth in the oasis regions begins to cause
401 establishment of the species.

402 Further illustration of the evolution of the population distribution over time and its
403 dependence on $\bar{r}$ is presented in Figure 5, in which, colorplots of the population density distribution
404 are presented at four different times. Two cases – $\bar{r} = 10$ (expected to cause extinction) and $\bar{r} =$
405 60 (expected to cause establishment) – are considered. The $\bar{r} = 10$ colorplots are characterized by

406 a continuous reduction in population density with time, despite a shift of the peak of the population
407 density from the initial region towards the two oasis regions as time passes. Mathematically, $\bar{r}$
408 represents the ratio of growth and diffusion terms, and, with $\bar{r} = 10$, the rate of growth in the oasis
409 regions is simply not sufficient to sustain the population and overcome boundary losses.
410 Eventually, at large times, the small amount of species still surviving is located predominantly at
411 the center of the domain, as far away as possible from the hostile boundaries.

412 In contrast, the evolution of population colorplots for the $\bar{r} = 60$ case is markedly different.
413 Colorplots presented in Figure 5 clearly show the population diffusing, first towards the circular
414 oasis, which is closer to the initial population region, followed by diffusion towards the elliptical
415 oasis at later times. At small times, there is actually a reduction in the maximum population density
416 due to diffusion of the initially dense population into a larger space. This dilution, however, is
417 eventually overcome by aggressive growth in the oasis regions due to the relatively large value of
418 $\bar{r}$, leading to establishment of the population. At $\tau = 0.28$, Figure 5 shows that the population is
419 concentrated mainly in the circular oasis, with a secondary concentration in the elliptical oasis.
420 Even though both oasis regions have the same growth coefficient, greater concentration in the
421 circular oasis is simply due to its closer proximity to the initial population region.

422 Finally, it is also of interest to track the population density at specific locations within the
423 space as functions of time. This is presented in Figure 6, which plots $\bar{c}$ at the centers of the circular
424 oasis and the initial population region as functions of time. Curves are presented for $\bar{r} = 10$ and
425 $\bar{r} = 60$ in Figures 6(a) and 6(b), respectively. The $\bar{r} = 10$ curves show that population density at
426 the center of the initial region decreases monotonically as the initial population diffuses out of the
427 initial region and does not grow sufficiently in the oasis region due to the relatively low value of
428 $\bar{r}$. The population density at the center of the circular oasis increases for some time, as it receives

429 population diffusing out of the initial region, However, such growth is not sustained for long due
430 to the stronger impact of diffusion and boundary loss compared to growth. Eventually, the
431 population density in the circular oasis also approaches extinction at large time. These observations
432 are consistent with other plots presented earlier in this section.

433 In contrast, as shown in Figure 6(b), when $\bar{r} = 60$, population density at the center of the
434 circular oasis continues to rise with time. While the growth is somewhat linear at small times,
435 eventually, as the population establishes itself firmly, the growth becomes much stronger.
436 Population density at the center of the initial population region exhibits an interesting bowl-shaped
437 curve. The initial reduction in population density is mainly due to diffusion away from the initial
438 population region. Slowly, as growth in the oasis regions becomes more and more dominant, a
439 plateau region occurs, where diffusion away from the initial region is balanced by increase in
440 population due to growth in the oasis regions and subsequent diffusion back into the initial
441 population region. Due to the large value of $\bar{r}$ in this case, population growth in the oasis regions
442 becomes more and more aggressive, and eventually, population density at both points shown in
443 Figure 6(b) begins to increase exponentially.

444 *4.3. Establishment-vs-Extinction Regimes*

445 It is of much interest to identify regions in the parameter space whether establishment or
446 extinction will occur at large times. For any given oasis region, its size and growth coefficient both
447 contribute towards population establishment. In order to examine the relationship between these
448 parameters and to identify establishment and extinction regions in the 2D parameter space defined
449 by these parameters, the minimum value of $\bar{r}$ needed for population establishment is determined
450 as a function of the radius of a circular oasis located at the center of a square-shaped space. The
451 initial population is assumed to be present uniformly throughout the two-dimensional space. For

each oasis radius, determinant of the matrix $\boldsymbol{M}$ is calculated for multiple values of $\bar{r}$, and the threshold value of $\bar{r}$ to ensure establishment is determined by examining where the determinant becomes zero. The resulting plot is presented in Figure 7. As expected, the larger the oasis radius, the smaller is the value of $\bar{r}$ needed for population establishment. Regions under and above the curve represent the extinction and establishment regimes, respectively. The relationship between $\bar{r}$ and oasis radius is not linear, however. Figure 7 shows that the requirement for $\bar{r}$ becomes quite steep in the small size limit, indicating that small oasis regions must have particularly large growth coefficients in order to ensure species establishment. In the other extreme, as the oasis size becomes very large and approaches the size of the region itself, the growth coefficient needed for establishment is no longer as sensitive to oasis size. In other words, once the oasis is sufficiently large, making it even larger does not significantly reduce the growth coefficient required for establishment.

While Figure 7 specifically addresses the interaction between oasis size and growth coefficient, relationships between other problem parameters, such as diffusion coefficient versus growth coefficient may also be examined similarly by determining extinction and establishment regions in the parameter space, based on the determinant approach for finding the threshold between extinction and establishment.

4.4. Illustrative Problems with Complicated Oasis and Initial Population Region Geometries

A key feature of the theoretical technique developed in this work lies in its capability to account for irregular shapes of oasis/deadzone regions that need not match the Cartesian nature of the two-dimensional space itself. The definition of the outer boundary of each region in terms of ξ_{1p} and ξ_{2p} in the ξ direction, and $\eta_{1p}(\xi)$ and $\eta_{2p}(\xi)$ in the η direction makes it possible to

consider a variety of possible shapes of each region, such as a circle or even other more complicated shapes. Two example problems are solved in order to illustrate this capability.

First, a problem is considered with a single oasis shaped like a heart. For a rectangular initial distribution of the population between $\xi = 0.05$ and $\xi = 0.95$, and between $\eta = 0.05$ and $\eta = 0.95$, Figure 8 plots the resulting population density distribution colormaps at multiple times. Other problem parameters are $\bar{D}_1 = 0.5$, $\bar{r}_1 = 40$, $\bar{r}_0 = 0$, $\bar{W} = 1$. An outline of the shape of the oasis is shown using dashed lines. Figure 8(a) shows that the population begins to concentrate in the heart-shaped oasis even at very early times. The shape of the population density is close to the shape of the heart itself in Figures 8(a) and 8(b). As time passes, the population distribution becomes more and more concentrated in regions away from the boundary due to the hostile nature of the boundary, and, specifically, the population density in the heart-shaped oasis continues to grow. On the overall, in this case, the growth phenomenon in the oasis dominates over population loss due to diffusion to hostile boundaries, and the population density is found to grow over time, while remaining concentrated within the oasis region. Note that the contours in the population colormap closely match the shape of the oasis at early times, but no longer at large times, due to the diffusive nature of population transport.

As another illustration, a problem is considered in which the population is initially placed in four leaf-shaped regions, while a circular oasis is also present. The locations and shapes of the initial regions and the oasis are shown in Figure 9 using dotted and dashed lines, respectively. Note that the oasis intersects partly with two of the leaf-shaped regions. Starting with a uniform initial population distribution in the leaf-shaped regions, the goal is to determine the population density colorplots at future times, and whether the population establishes itself or goes extinct. With $\bar{D}_1 = 1.5$, $\bar{r}_1 = 40$, $\bar{r}_0 = 5$, $\bar{W} = 1$ and a uniform initial population distribution in the leaf-shaped

regions, Figure 9 presents population distribution colorplots at multiple times for this problem. These plots show the population to be concentrated in the leaf-shaped regions initially and starting to diffuse outwards at early times. Between Figure 9(a) and 9(b), the peak population density actually reduces due to diffusion of the initially concentrated population density over a greater area. As time passes, Figure 9 shows a build up of population in the circular oasis, as expected due to the positive value of $\bar{r}_1 = 40$. At large times, the population is mainly concentrated in and around the circular oasis, and the peak concentration continues to increase, indicating establishment and exponential growth of the total population over time.

Figures 8 and 9 illustrate the capability of the exact theoretical technique developed here to analytically determine the population dynamics, while accurately accounting for complicated geometries of the oasis/deadzone regions as well as the initial population distribution. Note that the theoretical model is an exact analytical treatment of this problem and does not require spatial or temporal discretization commonly needed for numerical simulations.

4.5. Oasis and Deadzone Regions

The theoretical treatment presented in this work accounts for both positive and negative growth coefficients. $\bar{r} > 0$ indicates growth in the region, referred to as an oasis in this work. Conversely, $\bar{r} < 0$ inhibits growth and results in reduction in population, referred to as a deadzone in this work. It is of interest to examine the population dynamics in a scenario where both oasis and deadzone regions are present. In such a scenario, it is unclear whether the oasis or the deadzone dominates, leading to either establishment or extinction of the population. A representative problem with an oasis and a deadzone region is considered. Both regions are circular in shape, with the same radius of 0.15. The centers of the oasis and deadzone are located at $(0.20,0.50)$ and $(0.80,0.50)$, respectively. The values of the growth coefficient are $\bar{r}_1 = 100$ for the oasis and

$\bar{r}_2 = -100$ for the deadzone. The diffusion coefficient for the oasis and deadzone regions relative to the rest of the space is $\bar{D}_1 = 1.5$. The initial population region is a rectangle of size 0.2 by 0.2, located at the center of the two-dimensional space. For this problem, the population density distribution is computed as a function of time based on the theoretical model presented in Section 2. Results are presented in Figure 10 in terms of population density colormaps at four different times. The locations of the oasis and deadzone regions, as well as the initial population region are indicated in each colorplots. Figure 10(a) shows that at early times, the population diffuses outwards from the initial region in all directions. However, as time passes, there is preferential migration of population towards the oasis region, and away from the deadzone region. Comparing Figures 10(a) and 10(b), the peak population density reduces, which is because of diffusion of the initially concentrated population into a larger space. As time passes, the effect of growth in the oasis and annihilation in the deadzone can be clearly seen in Figures 10(b)-10(d). Specifically, the population density in the oasis continues to rise with time, whereas there is hardly any population remaining in the deadzone region at large times. On the overall, despite the same magnitude of the growth coefficient in the oasis and deadzone regions and despite their symmetric locations, the population on the overall is able to establish itself. The reason for the dominance of the oasis region over the deadzone is that the impact of the deadzone is spatially restricted and self-limiting – once the population density in the deadzone region is sufficiently small, it can no longer reduce the population density much, particularly in regions far away from the deadzone. In contrast, the oasis region is able to continue to grow the population, which then diffuses out of the oasis. As the population density in the oasis region grows, so does its rate of further growth. Figure 10 clearly shows the overall preference of the population to grow in and around the oasis, while avoiding the deadzone and region around the deadzone.

In order to further understand the nature of interaction between the oasis and deadzone regions, the total population in the space is plotted as a function of time in Figure 11. Curves are presented for the baseline case studied in Figure 10, for which, the growth coefficient are $\bar{r}_1 = 100$ for the oasis and $\bar{r}_2 = -100$ for the deadzone. Two other cases are also considered – $\bar{r}_1 = 100$ and $\bar{r}_2 = -200$, which considers an even stronger deadzone compared to the baseline, and $\bar{r}_1 = 50$ and $\bar{r}_2 = -100$, which considers a weaker oasis than the baseline. Figure 11 shows exponential population growth for the baseline case, which is consistent with the population density colormaps presented in Figure 10. Making the deadzone even stronger at $\bar{r}_2 = -200$ is found to result in only minor reduction in the population curve, which nevertheless grows exponentially, and leads to population establishment. In contrast, Figure 11 also shows that reducing the oasis growth coefficient to $\bar{r}_1 = 50$ dramatically changes the population dynamics, leading to extinction. This shows that the population dynamics in this problem is strongly dependent on the growth coefficient of the oasis, whereas the impact of the deadzone is relatively much weaker.

4.6. Impact of oasis diffusion coefficient

The diffusion coefficient is also an important parameter that governs the dynamics of population growth in this problem. While the diffusion coefficient of the region outside the oasis and deadzone regions, D_0, is used for non-dimensionalization, the diffusion coefficient of the oasis and deadzone regions is represented non-dimensionally by $\overline{D}_p$, the ratio of the diffusion coefficient of the p^{th} region and the background. $\overline{D}_p > 1$ and $\overline{D}_p < 1$ represent scenarios where species diffusion within the oasis occurs faster or slower, respectively, than outside.

564 Since $\overline{D}_p$ governs how well population diffusion occurs within the oasis region, therefore,
565 it is of interest to determine the impact of $\overline{D}_p$ on whether population establishment or extinction
566 occurs. In order to do so, a specific problem comprising a single circular oasis region of radius
567 0.15 centered at $(0.3,0.5)$ is considered. The population is located initially in a square region, as
568 shown in the inset in Figure 12. As the population density distribution evolves, Figure 12 plots the
569 total population as a function of time for multiple values of $\overline{D}_1$. This analysis is presented for two
570 different values of the growth coefficient $\bar{r}_1 = 40$ and $\bar{r}_1 = 10$ in Figures 12(a) and 12(b),
571 respectively. Figure 12(a) shows that small values of $\overline{D}_1$ result in exponential population growth
572 and rapid establishment. This is mainly because small diffusion coefficient within the oasis
573 prevents the population from exiting the oasis and facilitates even greater growth by keeping the
574 species concentration in the oasis high. As $\overline{D}_1$ is increased, Figure 12(a) shows that population
575 growth first slows down (for the $\overline{D}_1 = 0.15$ case), and then stops completely (for the $\overline{D}_1 = 0.5$ and
576 $\overline{D}_1 = 2.0$ cases), leading to extinction when $\overline{D}_1$ is relatively large. Note that even when species
577 establishment occurs (for the $\overline{D}_1 = 0.1$ and $\overline{D}_1 = 0.15$ cases), the exponential growth of population
578 is preceded by a small dip in population over a considerable time. This is mainly attributed to
579 species loss at the hostile boundaries before sufficient population has diffused to the oasis. As a
580 result, the growth effect of the oasis takes some time to begin to dominate. Until then, the total
581 population does not rise rapidly and even drops somewhat.

582 The dynamics of population growth are markedly different when the growth coefficient of
583 the oasis is relatively low, $\bar{r}_1 = 10$, as shown in Figure 12(b). Here, the growth effect due to the
584 oasis is not sufficiently large to overcome population loss due to diffusion to hostile boundaries.
585 In this regime, the population growth dynamics are not very sensitive to the value of $\overline{D}_1$. Even
586 when $\overline{D}_1$ is quite small, the total population goes extinct, because, even though the species is

sufficiently retained within the oasis due to low $\overline{D}_1$, the growth coefficient is too small to counteract population loss due to diffusion and hostile boundaries. Therefore, in this case, extinction occurs for each value of the diffusion coefficient considered.

5. Conclusions

This work extends the state-of-the-art in the mathematical analysis of population dynamics and establishment/extinction of a population. Compared to the existing literature, the main contribution of this work lies in accounting for irregular shapes of growth regions in a two-dimensional space. Most of the past work assumes Cartesian patches within a Cartesian space, whereas the present work makes it possible to account for growth in realistic but irregular shapes and predict whether population establishment or extinction occurs as a result.

The theoretical model developed here may be easily extended to account for a mixed boundary condition instead of the zero population boundary condition assumed here. In such a case, the eigenfunctions $f_n(\xi)$ and $g_m(\eta)$ are given by a linear combination of sine and cosine functions instead of a purely sinusoidal function, in accordance with the mixed boundary condition. Further, extension to account for advective transport of population, as may be the case for inspect populations [23], is also straightforward.

While developed in this work in the context of population dynamics, the theoretical technique may also find applications in other related problems such as the proliferation of cancer cells.

Statements and Declarations

Funding

The author declares that no funds, grants, or other support were received during the preparation of this manuscript.

Competing Interests

The author has no relevant financial or non-financial interests to disclose.

Author Contributions

Ankur Jain – Conceptualization, Methodology, Formal Analysis, Investigation, Data Curation, Visualization, Writing Original Draft, Review/Editing.

References

[1] F. Brauer, C. Castillo-Chávez, *Mathematical Models in Population Biology and Epidemiology*, 2nd Ed., Springer, 2011. ISBN: 978-1461416852

[2] N. Shigesada, K. Kawasaki, *Biological Invasions: Theory and Practice*, 1st Ed., Oxford University Press, 1997. ISBN: 978-0198548515

[3] E. Holmes, M. Lewis, J. Banks, R.R. Veit, 'Partial Differential Equations in Ecology: Spatial Interactions and Population Dynamics,' *Ecology*, **75**, pp. 17-29, 1994. DOI: 10.2307/1939378

[4] R. Cantrell, C. Cosner, *Spatial Ecology via Reaction-Diffusion Equations*, 1st Ed., Wiley, 2004. ISBN: 9780471493013

[5] W. Fagan, M. Lewis, M. Neubert, P. Van Den Driessche, 'Invasion theory and biological control,' *Ecol. Lett.*, **5**, pp. 148-157, 2002. DOI: 10.1046/j.1461-0248.2002.0_285.x

[6] M. Lewis, S. Petrovskii, J. Potts, *The Mathematics Behind Biological Invasions*, 1st Ed., Springer, 2016. ISBN: 978-3319320427

[7] F. Hilker, E. Liz, 'Threshold harvesting as a conservation or exploitation strategy in population management,' *Theor. Ecol.*, **13**, pp. 519–536, 2020. DOI: 10.1007/s12080-020-00465-8

[8] S. Aniţa, V. Capasso, S. Scacchi, *Mathematical Modeling and Control in Life and Environmental Sciences*, 1st Ed., Springer, 2024. DOI: 10.1007/978-3-031-49971-5

[9] J. Skellam, 'Random dispersal in theoretical populations,' *Biology*, **53**, pp. 135-165, 1991. DOI: 10.1016/S0092-8240(05)80044-8

[10] H. Kierstead, L. Slobodkin, 'The size of water masses containing plankton blooms,' *J. Marine Res.*, **12**, pp. 141-147, 1953.

[11] A. Okubo, *Diffusion and Ecological Problems: Mathematical Models*, 1st Ed., Springer-Verlag, 1980. ISBN: 978-3540096207.

[12] A. Lotka, 'Analytical Note on Certain Rhythmic Relations in Organic Systems,' *Proc. Nat. Acad. Sci. U.S.A.*, **6**, pp. 410–415, 1920. DOI: 10.1073/pnas.6.7.410

[13] V. Volterra, 'Fluctuations in the abundance of a species considered mathematically,' *Nature*, **118**, pp. 558-560, 1926. DOI: 10.1038/118558a0

[14] R. St. Clair, A, Nevai, R, Schugart, 'Reaction-diffusion model for population dynamics in patchy landscapes,' *J. Differential Eq.*, **405**, pp. 247-286, 2024.DOI: 10.1016/j.jde.2024.05.055

[15] R. Cantrell, C. Cosner, 'Diffusion models for population dynamics incorporating individual behavior at boundaries: applications to refuge design,' *Theor. Popul. Biol.*, **55**, pp. 189–207, 1999. DOI: 10.1006/tpbi.1998.1397

[16] A. Hastings, 'Transient dynamics and persistence of ecological systems,' *Ecol. Lett.*, **4**, pp. 215–220, 2001. DOI:10.1046/j.1461-0248.2001.00220.x

[17] R. Gatenby, E. Gawlinski, 'A reaction-diffusion model of cancer invasion,' *Cancer Res.*, **56**, pp. 5745-53, 1996.

[18] A. Jain, M. Parhizi, L. Zhou, G. Krishnan, 'Imaginary eigenvalues in multilayer one-dimensional thermal conduction problem with linear temperature-dependent heat generation,' *Int. J. Heat Mass Transf.*, **170**, pp. 120993:1-10, 2021. DOI: 10.1016/j.ijheatmasstransfer.2021.120993.

[19] A. Narasimhan, R. Rao, A. Jain, 'Theoretical and Simulation-Based Investigation of Heat Transfer and Thermal Runaway in Power MOSFET Devices,' *IEEE Trans. Components Packag. Manufac. Technol.*, in press, 2025. DOI: 10.1109/TCPMT.2024.3515012.

[20] Y. Chen, H. Xie, H. Ke, R. Chen, 'An analytical solution for one-dimensional contaminant diffusion through multi-layered system and its applications,' *Environ. Geol.*, **58**, pp. 1083–1094, 2009. DOI: 10.1007/s00254-008-1587-3

[21] A. Jain, S. McGinty, G. Pontrelli, L. Zhou, 'Theoretical Modeling of Endovascular Drug Delivery into a Multilayer Arterial Wall from a Drug-Coated Balloon,' *Int. J. Heat Mass Transf.*, **187**, pp. 122572:1-17, 2022. DOI: 10.1016/j.ijheatmasstransfer.2022.122572

[22] E. Bradford, J.R. Philip, 'Note on asocial populations dispersing in two dimensions,' *J. Theor. Biol.*, **29**, pp. 0022-5193. DOI: 10.1016/0022-5193(70)90116-5

[23] H. Banks, P. Kareiva, L. Zia, 'Analyzing field studies of insect dispersal using two-dimensional transport equations,' *Environ. Entom.*, **17**, pp. 815- 820, 1988. DOI: 10.1093/ee/17.5.815

[24] S. Berti, M. Cencini, D. Vergni, A. Vulpiani, 'Extinction dynamics of a discrete population in an oasis,' *Phys. Rev. E*, **92**, pp. 012722, 2015. DOI: 10.1103/PhysRevE.92.012722

[25] K. Owolabi, K. Patidar, 'Existence and Permanence in a Diffusive KiSS Model with Robust Numerical Simulations,' *Int. J. Diff. Eq.*, **2015**, pp. 485860:1-8, 2015. DOI: 10.1155/2015/485860

[26] C. Rao, P. Ren, Q. Wang, O. Buyukozturk, H. Sun, Y. Liu, 'Encoding physics to learn reaction–diffusion processes,' *Nature Machine Intelligence*, **5**, pp. 765–779, 2023. DOI: 10.1038/s42256-023-00685-7

[27] R. Cantrell, C. Cosner, 'The effects of spatial heterogeneity in population dynamics, ' *J. Math. Biol.*, **29**, pp. 315-338, 1991. DOI: 10.1007/BF00167155

[28] S. Levin, 'Population Dynamic Models in Heterogeneous Environments,' *Annu. Rev. Ecol. Evol. Systematics*, **7**, pp. 287-310, 1976. DOI: 10.1146/annurev.es.07.110176.001443

682 [29] H. Seno, ‘Effect of a singular patch on population persistence in a multi-patch system,’ Ecol.
683 Model., **43**, pp. 271-286, 1988. DOI: 10.1016/0304-3800(88)90008-7

684 [30] G. Maciel, F. Lutscher, ‘How individual movement response to habitat edges affects
685 population persistence and spatial spread,’ *Am. Nat.,* **182**, pp. 42–52, 2013. 10.1086/670661.

686 [31] M. Abramowitz, I. Stegun, *Handbook of Mathematical Functions*, United States Department
687 of Commerce National Bureau of Standards, 1964.

688 [32] Strang, G., *Introduction to Linear Algebra*, 5th Ed., Wellesley-Cambridge Press, 2016.

List of Figures

Figure 7. Extinction and establishment regimes in the parametric space of oasis radius and reaction coefficient for a problem with a single circular oasis at the center of a square region. The initial population is located uniformly throughout the square. Problem parameters are $\bar{D}_1 = 1.5$ and $\bar{W} = 1.0$.

Figure 8. Species establishment for an oasis with complicated geometry: Colormaps of population density distribution at multiple times for a problem with a heart-shaped oasis. Problem parameters are $\bar{D}_1 = 0.5$, $\bar{r}_1 = 40$, $\bar{r}_0 = 0$, $\bar{W} = 1$. The initial population density is distributed uniformly in the square region bounded by $\xi = 0.05$ and $\xi = 0.95$, and by $\eta = 0.05$ and $\eta = 0.95$. The oasis is shown using dashed lines.

Figure 9. Species establishment for a leaf-shaped initial population distribution and a circular oasis: Colormaps of population density distribution at multiple times. Problem parameters are $\bar{D}_1 = 0.5$, $\bar{r}_1 = 40$, $\bar{W} = 1$. The oasis and regions of initial population distribution are shown using dashed and dotted lines, respectively.

Figure 10. Population dynamics for a problem with one oasis and one deadzone: Population density distribution at four different times. The oasis and regions of initial population distribution are shown using dashed and dotted lines, respectively. The left circle is an oasis, while the right circle is a deadzone. Problem parameters are $\bar{r}_1 = 100, \bar{r}_2 = -100, \bar{D}_1 = \bar{D}_2 = 1.5, \bar{r}_0 = 0, \bar{W} = 1.5$. The oasis and regions of initial population distribution are shown using dashed and dotted lines, respectively.

Figure 11. Effect of relative strengths of oasis and deadzone coefficients in the problem considered in Figure 10: Total population as a function of time for three different pairs $(\bar{r}_1, \bar{r}_2)$.

Figure 12. Effect of oasis diffusion coefficient: Total population in the domain as a function of time for four different values of $\bar{D}_1$ for a problem with a single circular oasis region. (a) $\bar{r}_1 = 40$, (b) $\bar{r}_1 = 10$. Inset schematic shows the geometry, where the oasis is depicted with dashed lines, and the initial population region is depicted with dotted lines. Problem parameters are $\bar{r}_0 = 0, \bar{W} = 1.0$.

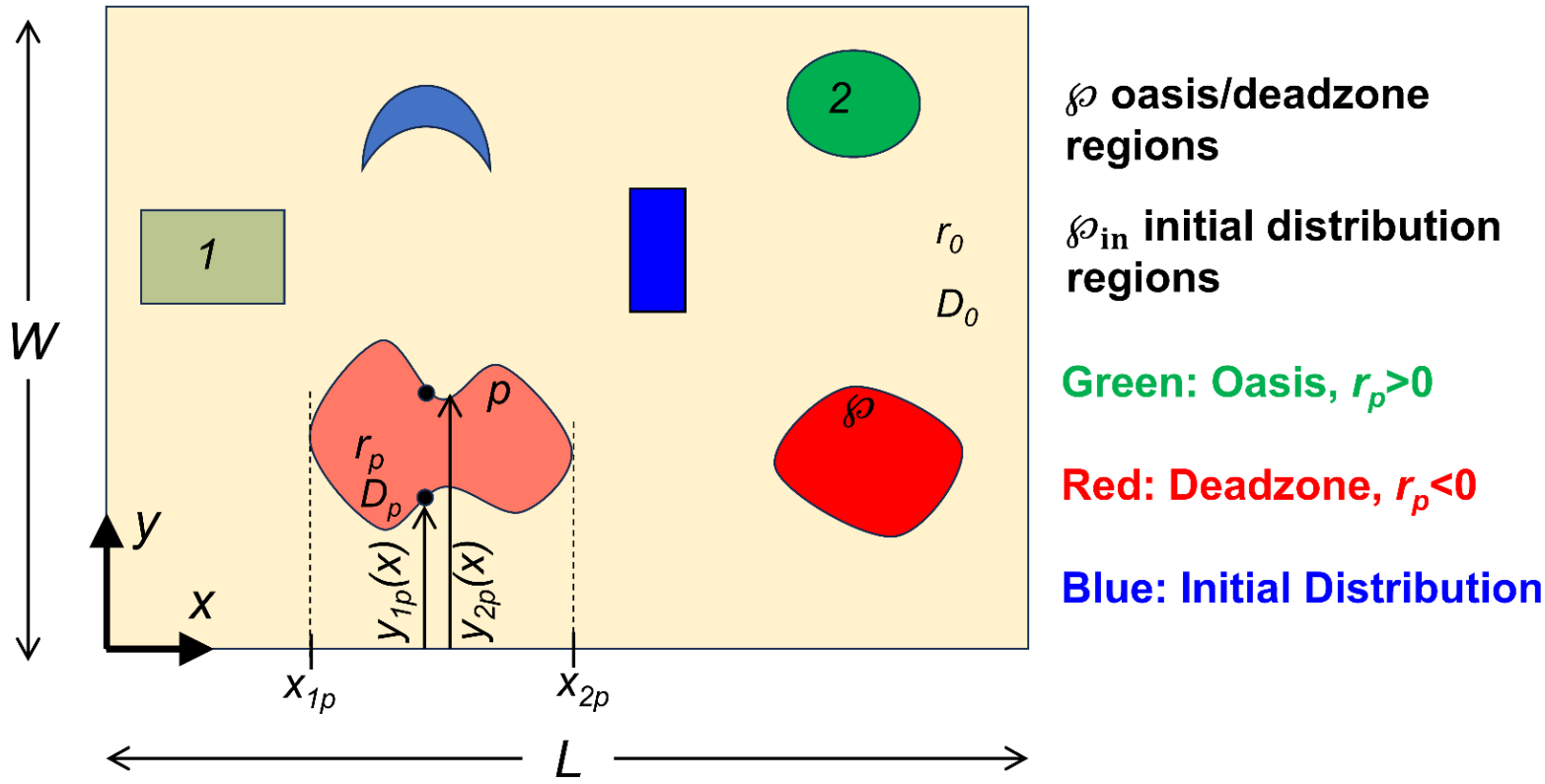

Figure 1. Schematic of the two-dimensional spatiotemporal population growth problem with irregularly-shaped regions that encourage (oasis) and discourage (deadzone) growth, as well as irregularly-shaped regions of the initial population. The shape of each region is mathematically described by lower and upper bounds x_1 and x_2, respectively, in the x direction, and lower and upper bounds $y_1(x)$ and $y_2(x)$.

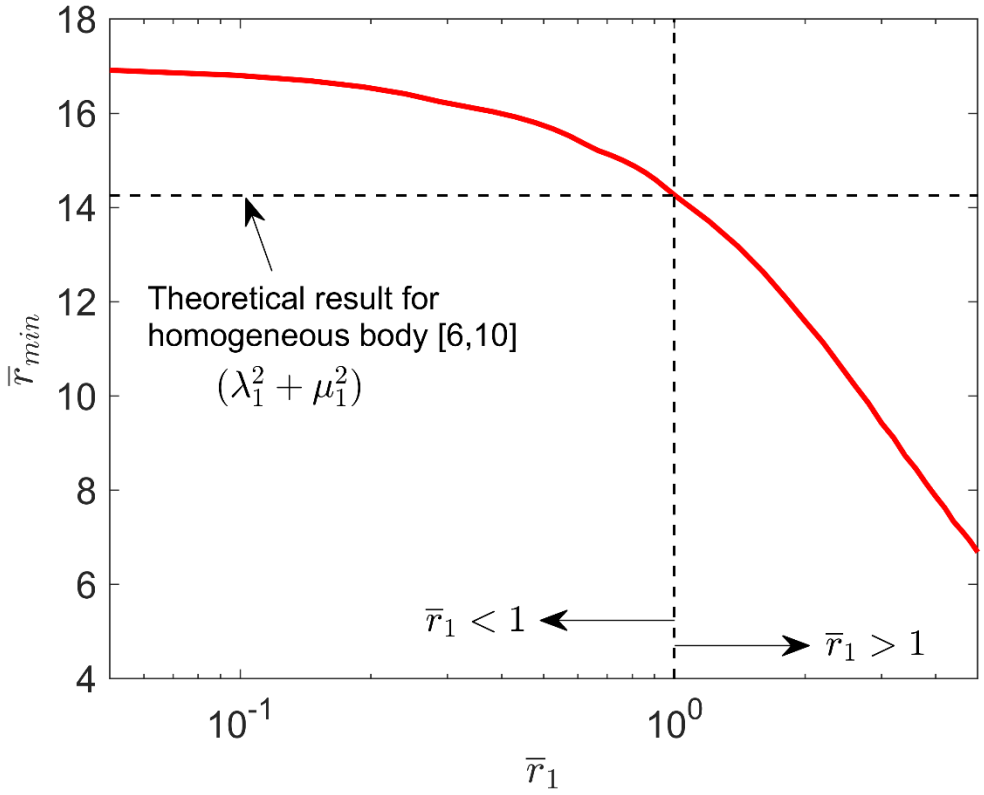

Figure 2. Minimum value of the growth coefficient $\bar{r}_{0,min}$ needed for population establishment as a function of $\bar{r}_1$, the ratio of growth coefficients inside and outside the oasis for a single circular oasis problem. The $\bar{r}_1 = 1$ limit, corresponding to a homogeneous space problem, is indicated by a vertical dashed line. The expected value of $\bar{r}_{0,min}$ based on past work [6,10] is also indicated by a horizontal dashed line. Problem parameters are $\bar{D}_1 = 1.0$ and $\bar{W} = 1.5$. The oasis of radius 0.2 is centered at $\xi = 0.7$ and $\eta = 0.7$.

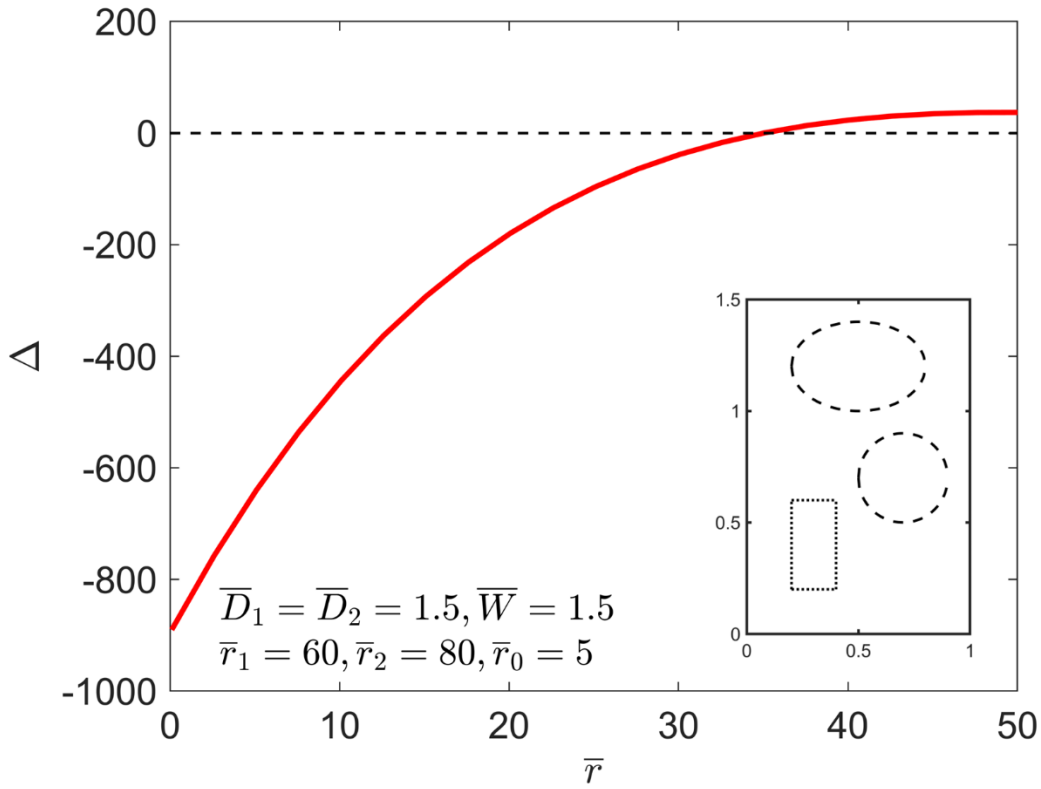

Figure 3. Determinant of matrix $\boldsymbol{M}$ as a function of $\bar{r}$ for a problem with circular and elliptical shaped oases, and a square shaped region of initial population, as specified in Section 4.2. Problem parameters are $\overline{D}_1 = \overline{D}_2 = 1.5$, $\bar{r}_0 = 5$, $\overline{W} = 1.5$. Both oases are assumed to have the same growth coefficient $\bar{r}$. Inset schematic shows the geometry, where the oases are depicted with dashed lines, and the initial population region is depicted with dotted lines.

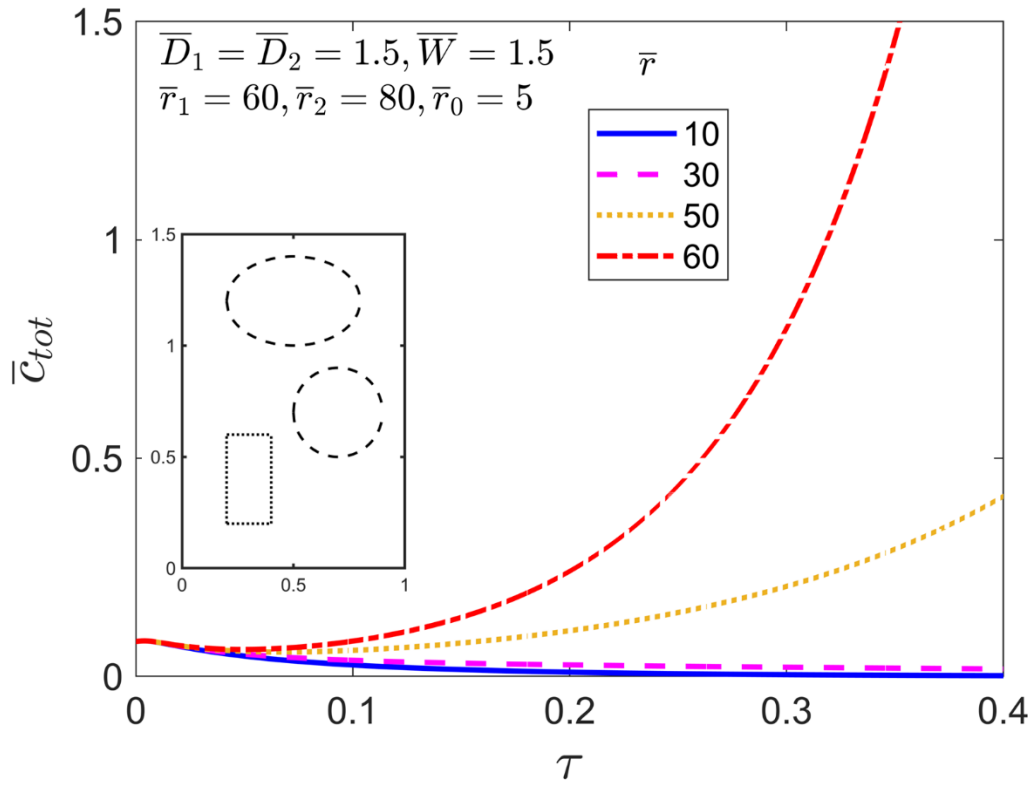

Figure 4. Total population as a function of time for four different values of $\bar{r}$ for the problem considered in Figure 3, showing species extinction for $\bar{r} = 10$ and $\bar{r} = 30$, and species establishment for $\bar{r} = 50$ and $\bar{r} = 60$.

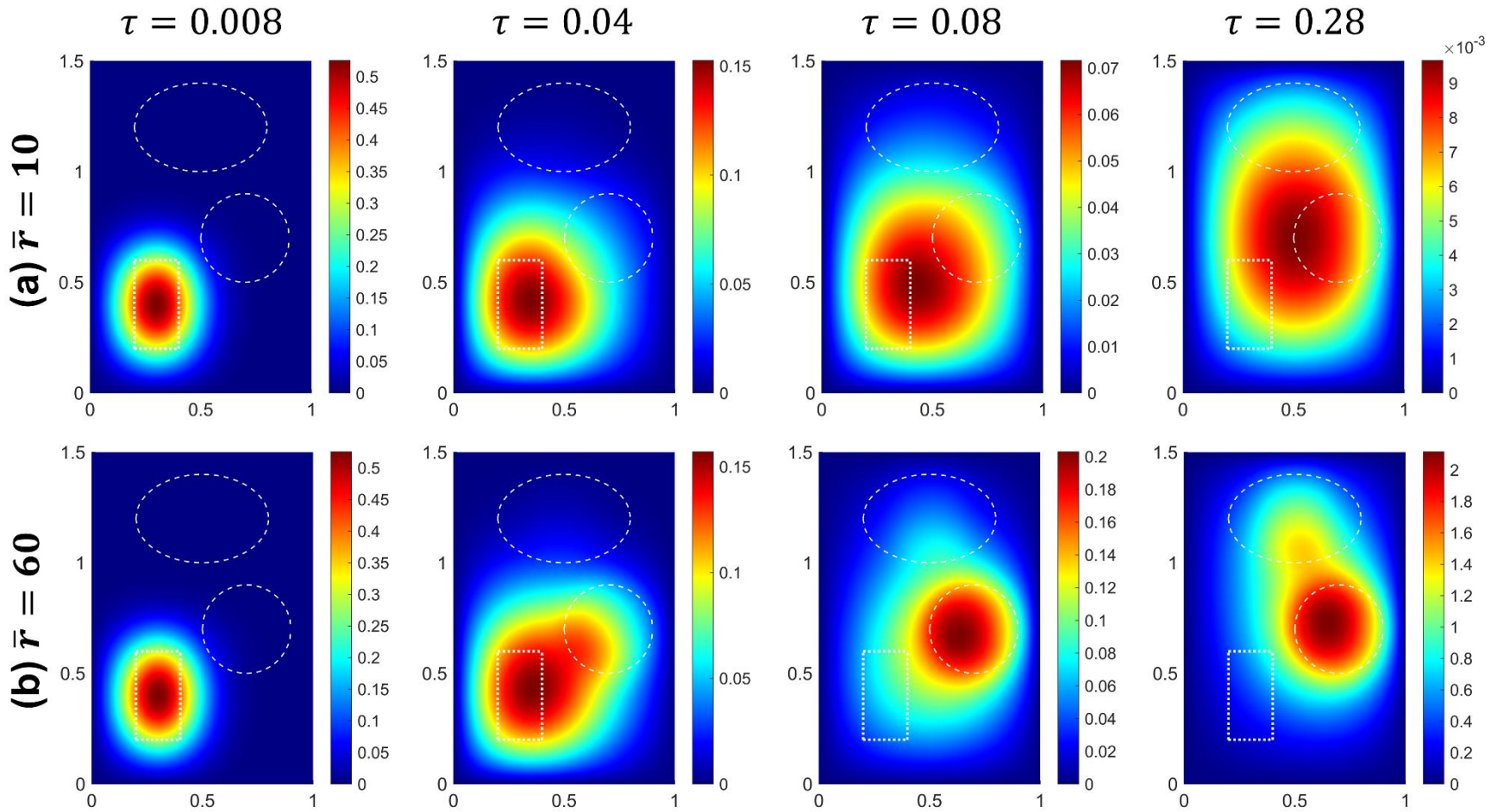

Figure 5. Colorplots of population density distribution at four different times for (a) $\bar{r} = 10$ and (a) $\bar{r} = 60$ for the problem considered in Figure 3.

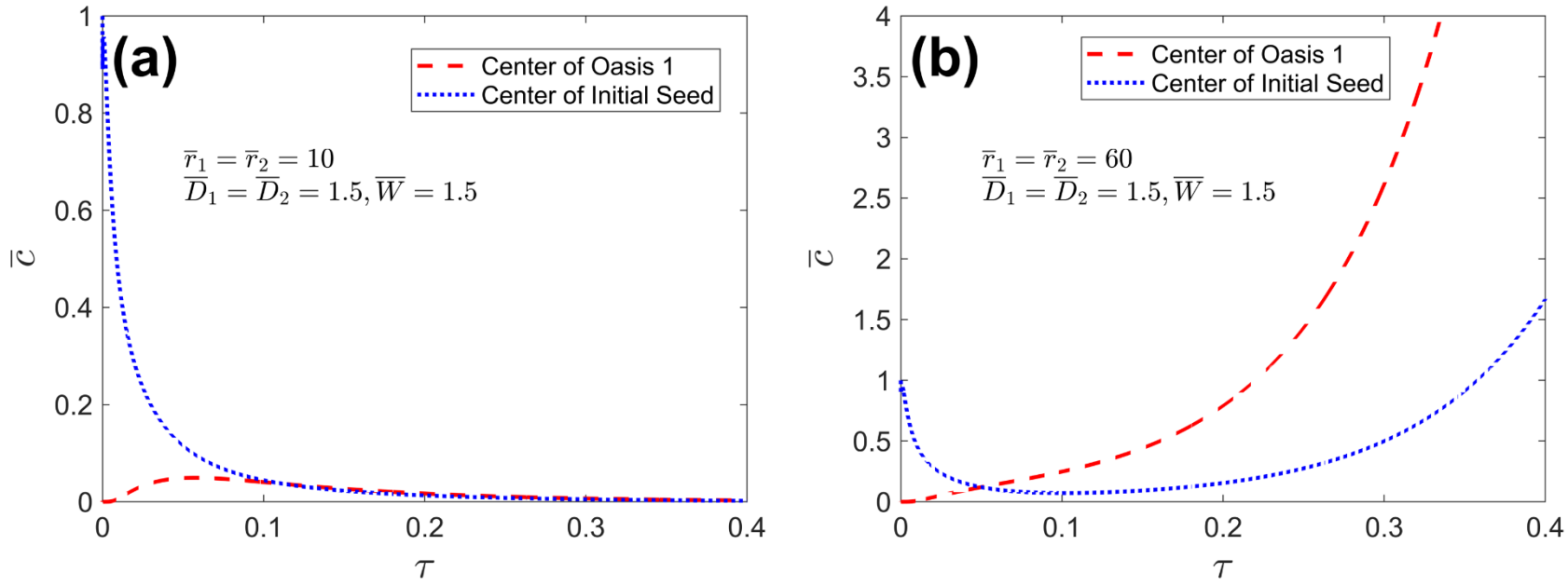

Figure 6. Population density at the centers of the first oasis and the initial population region as functions of time for (a) $\bar{r} = 10$ and (b) $\bar{r} = 60$ for the problem considered in Figure 3.

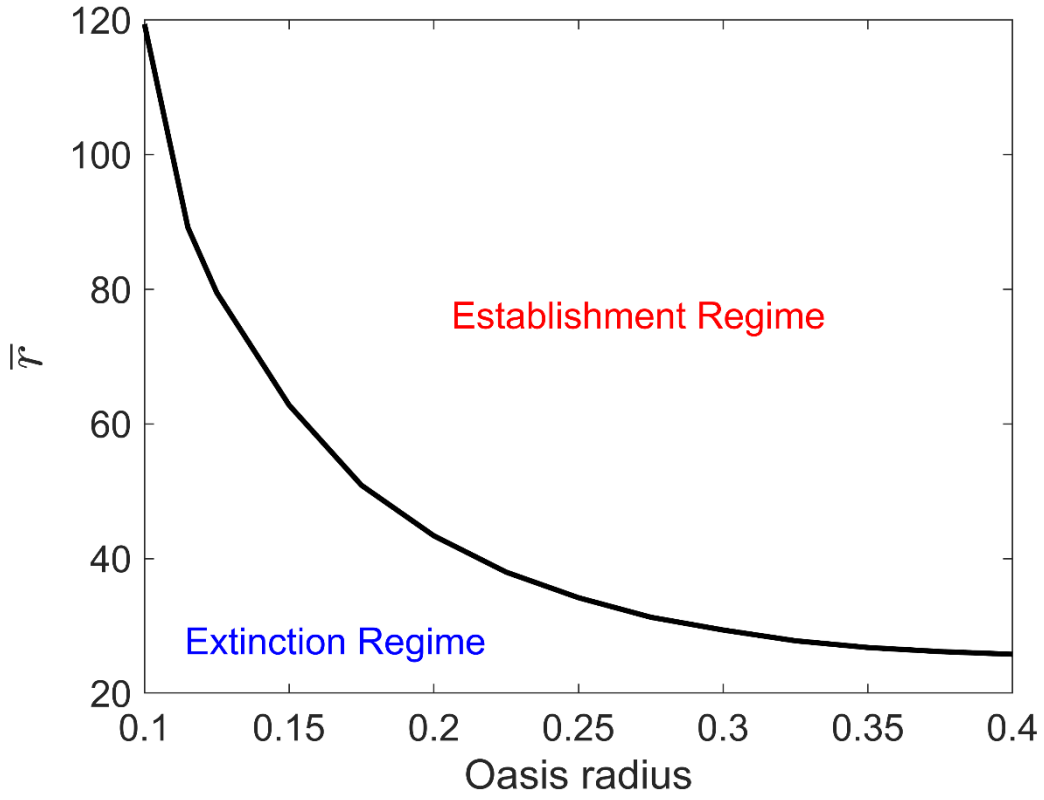

Figure 7. Extinction and establishment regimes in the parametric space of oasis radius and reaction coefficient for a problem with a single circular oasis at the center of a square region. The initial population is located uniformly throughout the square. Problem parameters are $\bar{D}_1 = 1.5$ and $\bar{W} = 1.0$.

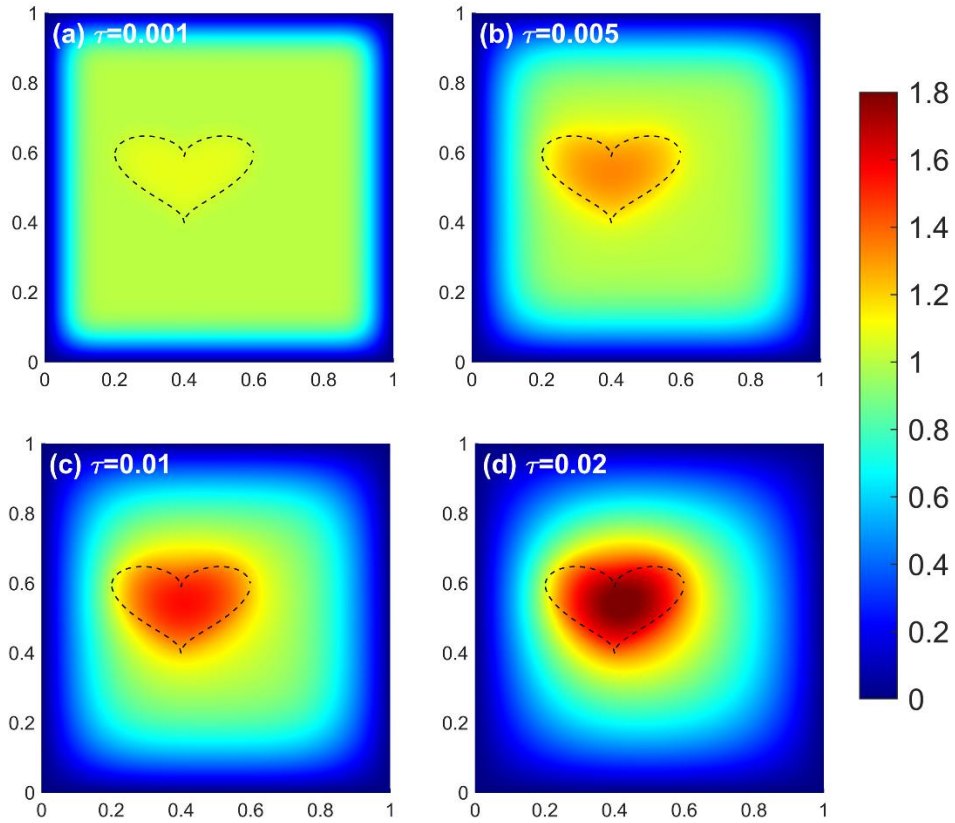

Figure 8. Species establishment for an oasis with complicated geometry: Colormaps of population density distribution at multiple times for a problem with a heart-shaped oasis. Problem parameters are $\bar{D}_1 = 0.5$, $\bar{r}_1 = 40$, $\bar{r}_0 = 0$, $\bar{W} = 1$. The initial population density is distributed uniformly in the square region bounded by $\xi = 0.05$ and $\xi = 0.95$, and by $\eta = 0.05$ and $\eta = 0.95$. The oasis is shown using dashed lines.

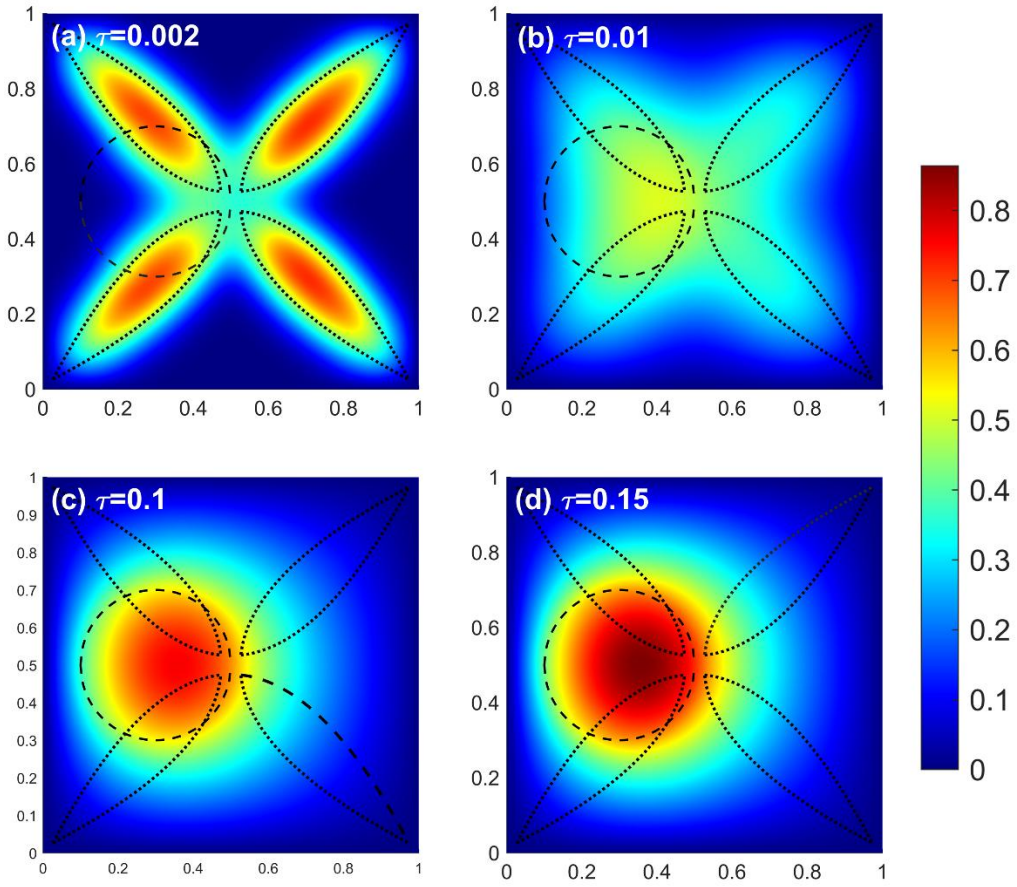

Figure 9. Species establishment for a leaf-shaped initial population distribution and a circular oasis: Colormaps of population density distribution at multiple times. Problem parameters are $\bar{D}_1 = 0.5$, $\bar{r}_1 = 40$, $\bar{W} = 1$. The oasis and regions of initial population distribution are shown using dashed and dotted lines, respectively.

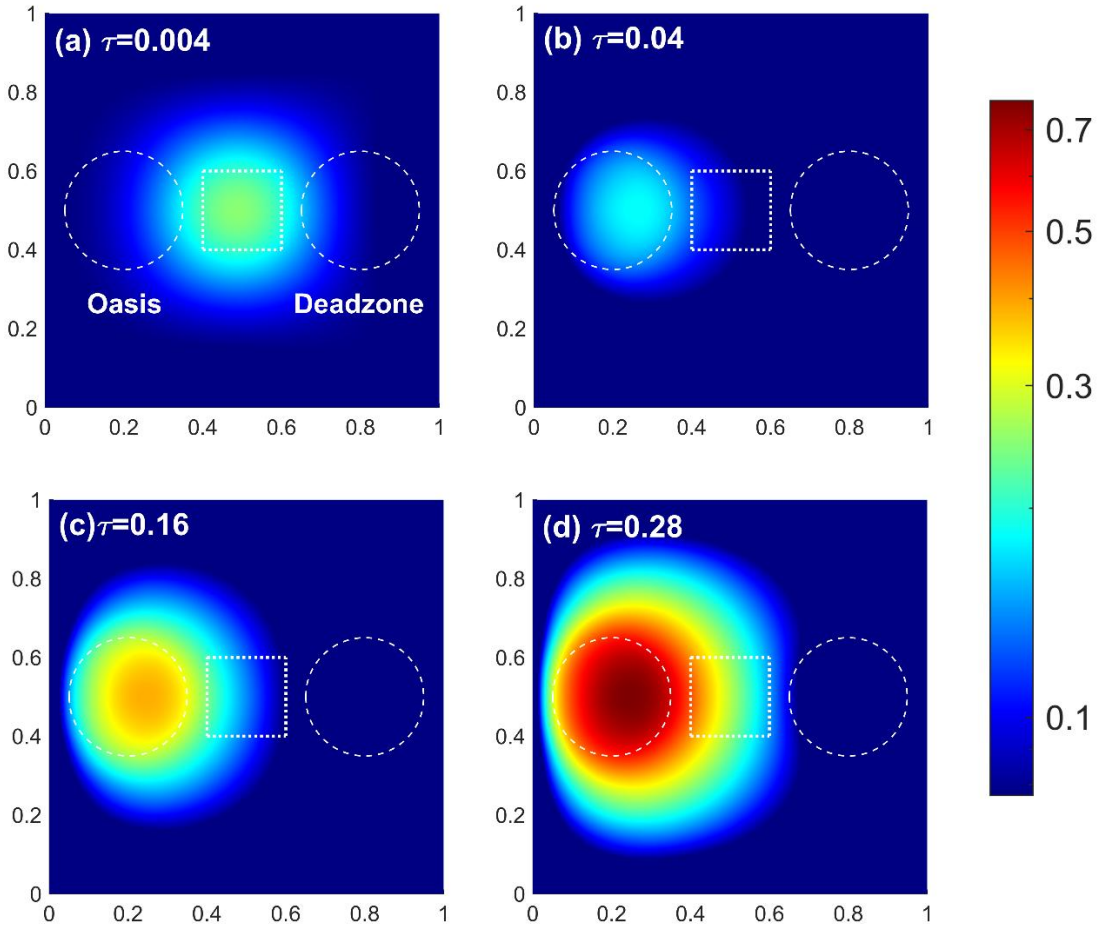

Figure 10. Population dynamics for a problem with one oasis and one deadzone: Population density distribution at four different times. The oasis and regions of initial population distribution are shown using dashed and dotted lines, respectively. The left circle is an oasis, while the right circle is a deadzone. Problem parameters are $\bar{r}_1 = 100, \bar{r}_2 = -100, \bar{D}_1 = \bar{D}_2 = 1.5, \bar{r}_0 = 0, \bar{W} = 1.5$. The oasis and regions of initial population distribution are shown using dashed and dotted lines, respectively.

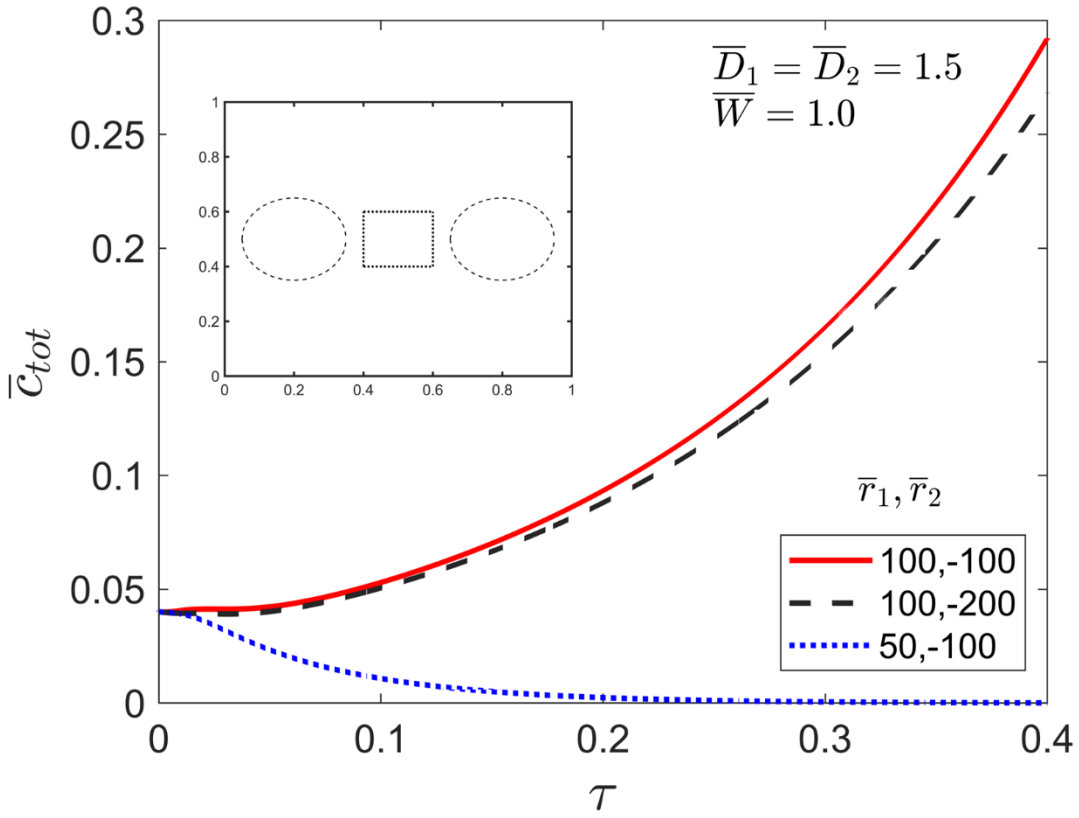

Figure 11. Effect of relative strengths of oasis and deadzone coefficients in the problem considered in Figure 10: Total population as a function of time for three different pairs $(\bar{r}_1, \bar{r}_2)$.

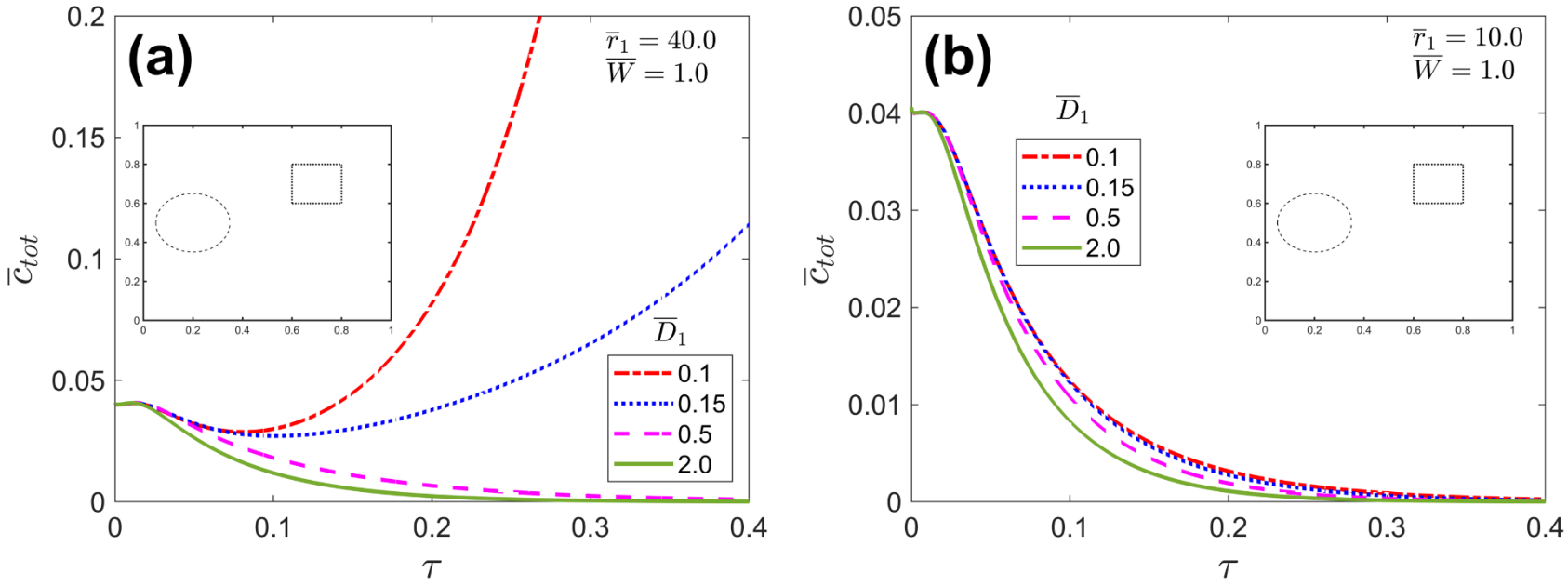

Figure 12. Effect of oasis diffusion coefficient: Total population in the domain as a function of time for four different values of $\bar{D}_1$ for a problem with a single circular oasis region. (a) $\bar{r}_1 = 40$, (b) $\bar{r}_1 = 10$. Inset schematic shows the geometry, where the oasis is depicted with dashed lines, and the initial population region is depicted with dotted lines. Problem parameters are $\bar{r}_0 = 0$, $\bar{W} = 1.0$.